Joint Special Interest Group meeting between euspen and ASPE
Advancing Precision in Additive Manufacturing
TU Berlin, Germany, October 2025
www.euspen.eu

Modeling the Interaction Effects of Laser Powder Bed Fusion Process Variables on Surface Texture to Enable Functional Tolerancing

M M Towfiqur Rahman[1], Chris J. Evans[1,2] Jason C. Fox[2], Jimmie Miller[1], Jaime Berez[1]

[1]Center for Precision Metrology, University of North Carolina at Charlotte, Charlotte, NC 28223, USA

[2]National Institute of Standards and Technology, Gaithersburg, MD 20899, USA

mrahma18@charlotte.edu

Abstract

Laser powder bed fusion (LPBF), a widely used metal additive manufacturing (AM) process, has diverse applications ranging from aerospace to biomedical, many of which require a comprehensive understanding of as-built surface topography to ensure that final parts meet their functional performance requirements, such as heat transfer efficiency and structural integrity. To optimize the performance of LPBF parts, functional tolerancing principles should be embraced, tailoring the relevant areal surface texture parameter specifications to the intended application. Meeting said specifications can be challenging, as a combination of interdependent process variables affects the surface topography of LPBF-produced parts. A significant gap remains in predictive modeling of surface texture: Existing studies rarely incorporate interaction or nonlinear effects of process variables, results are not always validated across a large process space, and simple roughness metrics (e.g., *Ra, Sa*) are primarily studied, overlooking more application-driven metrics (e.g., features, hybrid, functional, and spatial parameters). This study examines the surface texture of a large set of LPBF specimens, manufactured with varied laser power, scan speed, and hatch spacing. The ability of multiple models to predict surface texture is tested for a variety of parameters and filtering conditions. This work provides insights into the dependence of predictor significance on filter cutoff lengths. Additionally, this work shows the importance of not only the process variables of LPBF but also their interaction terms in producing a robust predictive model. Multiple possible predictive models for various areal surface parameters are also compared and contrasted.

Keywords: Laser powder bed fusion (LPBF), process parameters, predictive modeling, surface metrology

1. Introduction

Surface roughness is a crucial quality metric for any part, especially for parts produced with laser powder bed fusion (LPBF) due to its inherent roughness. Surface roughness of an LPBF part significantly impacts mechanical integrity, fatigue life, and tribological behavior [1–3]. Even with significant advancements, deterministic surface roughness analysis is still complex due to the stochastic behavior of LPBF surface topography [4,5].

According to Rehme and Emmelmann's estimation, the LPBF process has over 130 process variables, of which about 13 are crucial to the properties of the final part [6]. According to Ferrar et al., these crucial variables include laser power, scan speed, hatch spacing, oxygen concentration during processing, scanning strategy, laser beam diameter, and layer thickness [7].

These process variables greatly influence the areal surface texture of as-built parts, particularly power, scan speed, and hatch spacing. Surface topography has been the subject of numerous studies that have examined the effects of these variables both separately and in combination. For example, Cao et al. [8] showed that the interaction between laser power and scanning speed causes the most notable adverse effect on surface roughness. Additionally, there is a positive contribution rate from the interaction of scanning speed and layer thickness on surface roughness, indicating that controlling these process variables can enhance surface quality [8]. According to Calignano et al., scanning speed was the most significant influence on the surface roughness of LPBF components [9]. Jiang et al. investigated how laser power, scanning speed, and hatch spacing affected surface roughness, hardness, and density. According to their findings, laser power was the most crucial factor affecting every property they looked at [10].

Across multiple industries, the arithmetic mean of surface roughness, *Ra*, is still the widely used surface parameter to characterize the inherent surface roughness [11]. Many prior studies have proposed empirically formulated linear regression models to predict *Ra* or its areal equivalent, *Sa*, as a function of power, laser, and/or scan speed [12].

Though previous studies have reported regression coefficients as high as 98.9% [13], a significant research gap remains in the lack of model validation across multiple filter cutoff values, leaving the impact of scale changes on regression performance largely unexplored. Additionally, it is well established that roughness parameters such as *Ra* and *Sa* are insufficient to fully characterize the inherent surface features of as-built LPBF components [14]. Despite this, most existing literature focuses predominantly on *Ra, Rq* (the RMS average of roughness), *Sa*, or *Sq* (the areal RMS average) when examining the influence of process variables. For application-specific surface control, greater emphasis should be placed on other ISO 25178-2 areal parameters, including functional and hybrid metrics [15]. Moreover, the interaction effects among key process parameters—such as laser power, scan speed, and hatch spacing—are often neglected. This oversimplification restricts understanding of the complex mechanisms governing surface formation. The present study integrates scale-sensitive analysis, a broad range of areal parameters, higher-order interaction

modeling, and physically grounded interpretation within a robust factorial design framework to address these limitations.

2. Methodology

2.1 Manufacturing of LPBF specimens

LPBF specimens were manufactured with a selected range of possible machine parameters to effect surfaces displaying a diverse range of ISO 25178-2 parameters [15]. Power, laser scan speed, and hatch spacing were varied to meet this objective, keeping all other controllable process variables nominally constant.

Five levels of laser power, three levels of hatch spacing, and corresponding variations in three levels of scan velocities were selected to achieve volumetric energy density in the range of 60 to 130 J·mm^{-3}, which is known to yield sufficiently dense parts [16]. Table 1 presents the specific values of all the varied process variables of the specimen. These process variables were only varied for the final layer.

Table 1: Values of the varied process variables for specimen blocks.

Power (W)	Hatch spacing (mm)		
	0.11	0.15	0.20
	Scan velocity (mm/s)		
228	500, 600, 700	400, 500, 600	250, 310, 410
285	600, 700, 960	600, 650, 700	310, 410, 500
317	700, 960, 1200	600, 650, 700	410, 500, 600
370	700, 960, 1200	650, 700, 960	500, 600, 700

The individual specimens (shown in outlined yellow in Fig. 1) were fabricated on three super specimens (shown in outlined red in Fig. 1). Each super specimen was designed with a distinct hatch spacing, and each specimen had varying levels of power and scan speed, as specified in Table 1. Individual specimens measured 7 mm × 7 mm, while the super specimens were 53 mm × 29 mm. All three super specimens were built on a 101.6 mm × 101.6 mm build plate. The overall height of a super specimen was 12.70 mm, and the individual specimen height was 7.16 mm from the pedestal. The specimens were manufactured with Nickel superalloy 625 (INCONEL-625). A commercial EOS M290 machine at the NIST facility in Gaithersburg, MD, USA, was used to manufacture them.

2.2 Surface metrology of LPBF specimens

The additively manufactured specimens were characterized using a coherence scanning interferometer (CSI) (ZeGage Pro HD, Zygo Corp.). Surface parameters were computed using the integrated Mx™ software. A 5.5× Michelson objective yielded a lateral sampling interval of 1.47 µm/pixel and 2.50 mm × 1.88 mm field of view (from camera). Multiple fields of view were stitched together with a 20% overlap and adaptive adjust, a sub-pixel stitching algorithm to measure a single specimen. A 3×3 Gaussian denoise filter was initially applied to the raw surface data to reduce measurement noise. Subsequent preprocessing included planar form removal and 3.2σ outlier elimination, where σ is the multiplier used in the sigma-clipping function to discard extreme height deviations. The resulting S-F surfaces—primary surfaces with form removed using the F-operation defined in ISO 25178-2—were subjected to high-pass robust Gaussian filtering with three different cutoff lengths (λc), 0.08 mm, 0.25 mm, and 0.80 mm, as suggested by ASME B46.1-2019 further analysis [17]. Measurements were acquired from a 3.50 mm x 3.50 mm evaluation area from the center of the specimen to avoid local variations in surface texture near the rapid turnaround regions at the edges of specimens [18].

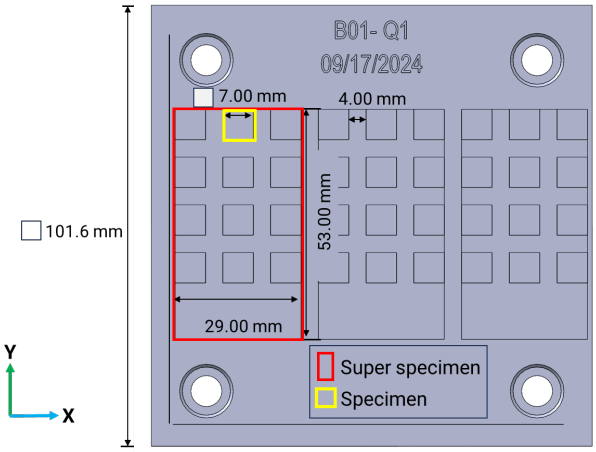

Figure 1. Positions and dimensions of the specimen and the master-specimen: red region indicates a super specimen (53 mm x 29 mm), while yellow indicates an individual specimen (7 mm x 7 mm).

2.3 Statistical analysis

The process of empirical modeling started with choosing a functional application for the surface and the relevant areal surface parameters – heat transfer was used as a case study. *Sdr* (developed interfacial area ratio of the scale-limited surface), *Sdq* (root mean square gradient of the surface), *Vmp* (peak material volume), *and Sk* (core roughness depth) were parameters hypothesized to dictate surface heat transfer efficiency and were selected to be studied as the response variables. Then, the varied LPBF process variables and their interaction terms were initially used to fit a least squares model using JMP® Data Analysis Software, following the procedures outlined in the JMP documentation [19]. Once it was found that no reliable linear regression model could be produced, predictive modelling was used for the chosen areal surface parameters. Before selecting the appropriate predictive model, the predictor screening feature in JMP was used to evaluate the significance of various predictors based on their potential to explain the response variable. This screening process employs bootstrap forest partitioning as its underlying methodology. In this approach, partition models are built using multiple predictors simultaneously, which enables the identification of variables that may have minimal individual effects but demonstrate significant influence when interacting with other predictors [20]. Once the significant predictors were identified, the surface parameter values for three different cutoffs were used in the model screening function of JMP software to identify which modeling approach was best suited to establishing a meaningful statistical relationship among the surface parameters and the process variables.

3. Results and discussions

The five above-mentioned areal surface texture parameters were first screened with eight predictors: power, velocity, hatch spacing, their interaction terms, and volumetric energy density (VED). Among the five areal parameters, *Sa*, *Sk*, and *Vmp* showed that interaction terms were essential in their prediction models. Interestingly, it was observed that the significant contributions of the predictors change depending on the applied cutoff lengths. For example, when a 0.80 mm cutoff length was used in the predictor screening of *Sa*, the major contributor was the interaction term of power and hatch spacing. When the cutoff length was 0.25 mm, the major model predictor changed to the interaction term of laser speed and hatch spacing, which

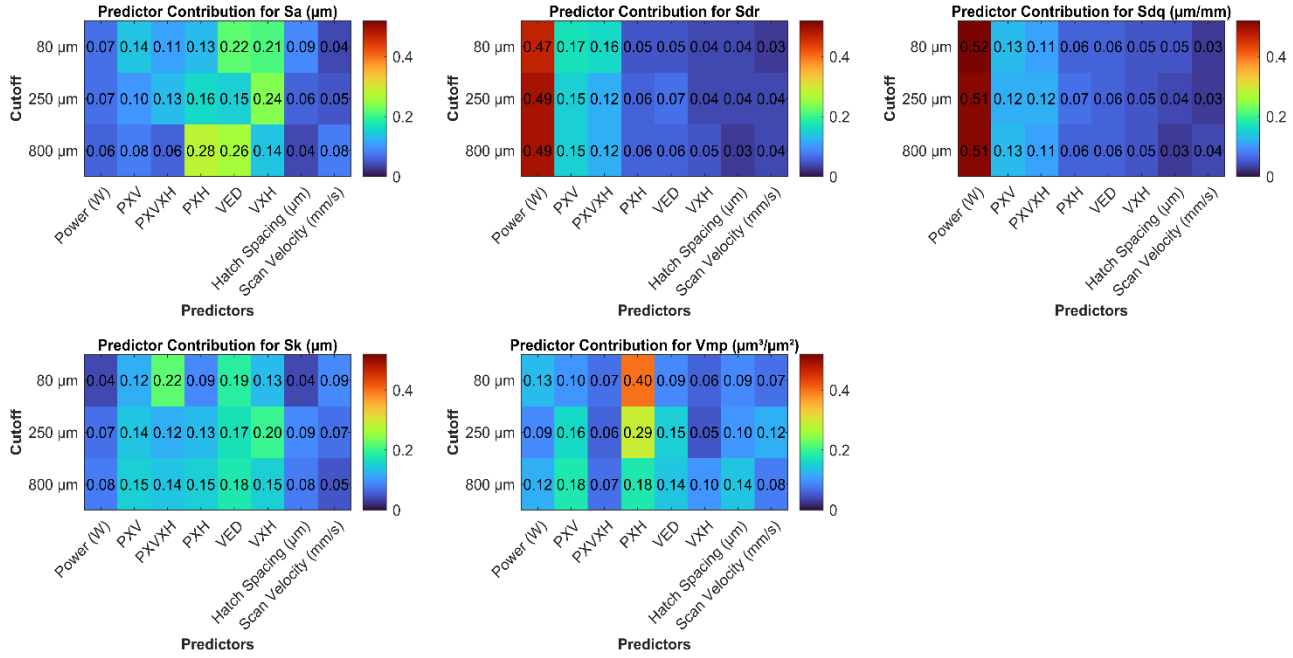

Figure 2. Predictor contributions for the five areal surface parameters with three different filter cutoff lengths.

implies that stating whether a particular process variable or any interaction term of process variables is significant or not depends on the filter cutoffs and should not be generalized across different length scales. Only *Sdr* among the five areal parameters showed consistency of process variables and their interaction terms regardless of filter cutoff lengths, making *Sdr* a distinctive areal parameter for mathematical modeling.

Among the independent process variables, hatch spacing and scan velocity were comparatively weak contributors for all five areal parameters across all different cutoff lengths (Figure 2).

Once significant predictors were chosen on a case-by-case basis for a combination of specific cutoff and areal surface parameters, they were used to model the surface parameters via model screening. Multiple models were investigated for model screening: neural boosted, partial least squares, generalized regression lasso, support vector machines, bootstrap forest, and boosted trees. Apart from the *Sdq* parameter's value with 0.25 mm cutoff length and the *Sk* parameter's value with 0.80 mm cutoff length, the neural boosted model showed the highest regression coefficient values, and the least root mean squared error among all other models. Bootstrap random forest was the best-performing model to predict the *Sdq* and *Sk* parameter values with 0.25 mm and 0.80 mm cutoffs, respectively. Table 2 shows the R^2 values for the areal surface parameters with the best-performing predictive model. For all the cases in Table 2 and all cutoffs, k-fold cross-validation was performed, with 80% of the data used to train the model and 20% used to validate it. As the dataset utilized was relatively sparse (N=36) for multiple cases, the results presented herein should not be generalized conclusively until more data can be acquired for additional model training and validation. Across all surface parameters, the R^2 values were consistently higher for the training data than the validation dataset, indicating the limitation of the small sample size. The influence of the filter cutoff lengths on prediction accuracy was also observed, suggesting that the model's accuracy depends on the retained surface features after filtering. The current data set shows that among the five surface parameters analyzed, *Sdr* showed the best predictive performance at the 0.80 mm cutoff (R^2 = 90% training, 60% validation), highlighting the importance of large-scale surface features. *Sdq* demonstrated a steady increase in validation accuracy as the cutoff increased, peaking at 70% at 0.80 mm, despite its training R^2 declining, which suggests better generalization at coarser scales. A maximum validation R^2 of 74% at 0.80 mm and low training R^2 values throughout made it challenging to model *Sk* consistently, suggesting model instability. *Sa* displayed inconsistent patterns with declining training performance; its best validation R^2 (77%) at λc = 0.25 mm indicated better generalization at mid-scale filtering. Training and validation R^2 values (42–67%) are balanced and moderate. With moderate and balanced training and validation R^2 values (42–67%), *Vmp* was the most resilient across all cutoffs, suggesting scale-insensitive predictability.

4. Conclusion

This study demonstrated the influence of process variables and their interaction terms on areal surface parameters. It emphasized that **predictors may be wrongly excluded if multiple surface filter cutoffs are not considered.** The significance of LPBF process variables and their interactions varied with cutoff length. This work also **extended predictive modeling** to additional areal parameters beyond common ones like *Ra* and *Sa*. It highlighted the value of multiple model screening and filter cutoffs to capture LPBF's complex process behavior and surface topologies. The limitation of this work is the sample size of the dataset; having a larger sample size would create a more meaningful or robust predictive model for the chosen areal surface parameters. Future work needs to be continued on this pursuit to capture as many individual process variables of LPBF as possible and their interaction terms to model various areal surface parameters so that the LPBF surfaces can be tuned with higher confidence according to their desired functionalities.

Table 2: Coefficient of regression (R^2) values for the five areal surface parameters across different filter cutoffs. R^2 values for *Sk* at the 0.08 mm cutoff and *Sdq* at the 0.25 mm cutoff were obtained using bootstrap random forest models. All other R^2 values correspond to predictions from the neural boosted network, identified as the best-performing model overall.

Cutoffs	R^2 value for 0.08 mm (%)		R^2 value for 0.25 mm (%)		R^2 value for 0.80 mm (%)	
Parameters	**Training**	**Validation**	**Training**	**Validation**	**Training**	**Validation**
Sdr	82	30	81	31	90	60
Sdq	81	44	66		37	70
Sk	38		31	26	23	74
Sa	81	29	43	77	22	61
Vmp	42	65	49	67	64	42

References

[1] Yang T, Liu T, Liao W, MacDonald E, Wei H, Chen X, et al. The influence of process parameters on vertical surface roughness of the AlSi10Mg parts fabricated by selective laser melting. Journal of Materials Processing Technology 2019;266:26–36. https://doi.org/10.1016/j.jmatprotec.2018.10.015.

[2] Vayssette B, Saintier N, Brugger C, El May M. Surface roughness effect of SLM and EBM Ti-6Al-4V on multiaxial high cycle fatigue. Theoretical and Applied Fracture Mechanics 2020;108:102581. https://doi.org/10.1016/j.tafmec.2020.102581.

[3] Delgado J, Ciurana J, Rodríguez CA. Influence of process parameters on part quality and mechanical properties for DMLS and SLM with iron-based materials. Int J Adv Manuf Technol 2012;60:601–10. https://doi.org/10.1007/s00170-011-3643-5.

[4] Nagamatsu H, Sasahara H, Mitsutake Y, Hamamoto T. Development of a cooperative system for wire and arc additive manufacturing and machining. Additive Manufacturing 2020;31:100896. https://doi.org/10.1016/j.addma.2019.100896.

[5] Dejene ND, Lemu HG, Gutema EM. Effects of process parameters on the surface characteristics of laser powder bed fusion printed parts: machine learning predictions with random forest and support vector regression. Int J Adv Manuf Technol 2024;133:5611–25. https://doi.org/10.1007/s00170-024-14087-5.

[6] Rehme, Olaf and Emmelmann, Claus. Reproducibility for properties of selective laser melting products, n.d.

[7] Ferrar B, Mullen L, Jones E, Stamp R, Sutcliffe CJ. Gas flow effects on selective laser melting (SLM) manufacturing performance. Journal of Materials Processing Technology 2012;212:355–64. https://doi.org/10.1016/j.jmatprotec.2011.09.020.

[8] Cao L, Li J, Hu J, Liu H, Wu Y, Zhou Q. Optimization of surface roughness and dimensional accuracy in LPBF additive manufacturing. Optics & Laser Technology 2021;142:107246. https://doi.org/10.1016/j.optlastec.2021.107246.

[9] Calignano F, Manfredi D, Ambrosio EP, Iuliano L, Fino P. Influence of process parameters on surface roughness of aluminum parts produced by DMLS. Int J Adv Manuf Technol 2013;67:2743–51. https://doi.org/10.1007/s00170-012-4688-9.

[10] Jiang H-Z, Li Z-Y, Feng T, Wu P-Y, Chen Q-S, Feng Y-L, et al. Factor analysis of selective laser melting process parameters with normalised quantities and Taguchi method. Optics & Laser Technology 2019;119:105592. https://doi.org/10.1016/j.optlastec.2019.105592.

[11] Todhunter LD, Leach RK, Lawes SDA, Blateyron F. Industrial survey of ISO surface texture parameters. CIRP Journal of Manufacturing Science and Technology 2017;19:84–92. https://doi.org/10.1016/j.cirpj.2017.06.001.

[12] Whip B, Sheridan L, Gockel J. The effect of primary processing parameters on surface roughness in laser powder bed additive manufacturing. Int J Adv Manuf Technol 2019;103:4411–22. https://doi.org/10.1007/s00170-019-03716-z.

[13] Safdar A, He HZ, Wei L, Snis A, Chavez De Paz LE. Effect of process parameters settings and thickness on surface roughness of EBM produced Ti-6Al-4V. Rapid Prototyping Journal 2012;18:401–8. https://doi.org/10.1108/13552541211250391.

[14] Pawlus P, Reizer R, Wieczorowski M. Functional Importance of Surface Texture Parameters. Materials 2021;14:5326. https://doi.org/10.3390/ma14185326.

[15] ISO 25178-2: Geometrical product specifications (GPS) — Surface texture: Areal Part 2: Terms, definitions and surface texture parameters 2021.

[16] Caiazzo F, Alfieri V, Casalino G. On the Relevance of Volumetric Energy Density in the Investigation of Inconel 718 Laser Powder Bed Fusion. Materials 2020;13:538. https://doi.org/10.3390/ma13030538.

[17] ASME. B46.1-2019 2019.

[18] M M Towfiqur Rahman, Chris J. Evans, Jason C. Fox, Jimmie Miller, Jaime Berez. Specification and Characterization of Laser Powder Bed Fusion Surfaces Textures for Heat Transfer in Internal Channels. ASPE-EUSPEN, 2024.

[19] JMP Documentation n.d.

[20] Predictor Screening 2024.